

# Identification of Septins in Neurofibrillary Tangles in Alzheimer's Disease

Ayae Kinoshita,\* Makoto Kinoshita,<sup>†</sup> Haruhiko Akiyama,<sup>§</sup> Hidekazu Tomimoto,\* Ichiro Akiguchi,\* Sharad Kumar,<sup>¶</sup> Makoto Noda,<sup>†</sup> and Jun Kimura\*

From the Departments of Neurology\* and Molecular Oncology,<sup>†</sup> Kyoto University Graduate School of Medicine, Yoshida Konoe-cho, Sakyo-ku, Kyoto, Japan; the Department of Neuropathology,<sup>§</sup> Tokyo Institute of Psychiatry, Tokyo, Japan; and the Hanson Centre for Cancer Research,<sup>¶</sup> Institute of Medical and Veterinary Science, Adelaide, Australia

**Septins are evolutionarily conserved cytoskeletal GTPases that can form heteropolymer complexes involved in cytokinesis and other cellular processes. We detected expression of the human septin genes *Nedd5*, *H5*, *Diff6*, and *hCDC10* in postmortem brain tissues using the reverse transcription-coupled polymerase chain reaction and their products by immunoblot analysis. Four antibodies directed against three septins, *Nedd5*, *H5*, and *Diff6*, consistently labeled neurofibrillary tangles, neuropil threads, and dystrophic neurites in the senile plaques in brains affected by Alzheimer's disease but did not label obvious structures in young control brains. Immunoelectron microscopy revealed that *Nedd5* localized to the paired helical filaments. Pre-tangles, the precursory granular deposits that accumulate in the neuronal cytoplasm, also were labeled with the antibodies. These findings suggest that at least the three septins are associated with tau-based paired helical filament core, and may contribute to the formation of neurofibrillary tangle as integral constituents of paired helical filaments. (Am J Pathol 1998, 153:1551-1560)**

Alzheimer's disease (AD) is a group of neurodegenerative disorders of multiple pathogeneses. The histopathology of the AD brain is characterized by profound neuronal loss and two distinct pathological features: senile plaques and neurofibrillary changes including neurofibrillary tangles (NFTs), neuropil threads, and dystrophic neurites in the senile plaques.<sup>1</sup> The number of NFTs correlates with the severity of dementia,<sup>2,3</sup> indicating a positive role for NFT in the functional disturbance of tangled neurons. As exemplified by transgenic mice that overexpress one of the neurofilament subunits,<sup>4,5</sup> excessive cytoplasmic deposit of certain proteins can disturb neuronal homeostasis, resulting in acceleration of the degenerative processes. This may also be true with AD

brains, in which NFTs progressively displace the normal neuronal cytoskeleton. Recent genetic approaches have revealed a number of key molecules for the pathogenesis of AD, ie, amyloid  $\beta$ -protein precursor ( $\beta$ PP), presenilins, and apolipoprotein E4.<sup>6</sup> So far, however, causal roles of these molecules in NFT formation have yet to be established.

NFT consists of a variety of abnormal filamentous structures represented by paired helical filaments (PHFs) 8–20 nm in diameter with a helical periodicity of 80 nm.<sup>7</sup> PHF is also the common structural basis of neuropil threads and a subset of dystrophic neurites in the senile plaque.<sup>8</sup> PHF is a heteropolymer complex of polypeptides, a major constituent of which is a microtubule-associated protein, tau. The presence of tau in NFT/PHF has been established by immunochemical analyses of brain tissues<sup>9–11</sup> and sequencing of PHF-derived peptides.<sup>12–14</sup> This structural heterogeneity of PHFs *in vivo* is attributable to biochemical modifications of tau<sup>15–17</sup> and/or involvement of other components.

Septins comprise a novel class of the GTPase family originally identified in the budding yeast mutants *CDC3*, *CDC10*, *CDC11*, and *CDC12*, which are commonly defective in cytokinesis.<sup>18,19</sup> The yeast septin gene products are the major constituents of the ~10-nm filaments formed beneath the plasma membrane at the mother-bud neck.<sup>20,21</sup> In *Drosophila*, at least three septins are concentrated near the contractile ring and in the nervous system as heteropolymer complexes.<sup>22–24</sup> In mammals, at least seven septin genes have been reported to date: *Diff6*,<sup>25</sup> *H5*,<sup>26</sup> and *Nedd5*<sup>27,28</sup> in the mouse and *hCDC10*,<sup>29</sup> KIAA0129, KIAA0158,<sup>30</sup> and *CDCrel-1*<sup>31</sup> in humans. Our database search and expression analyses revealed that (1) the counterparts of mouse *Diff6* and *H5* are expressed in humans, (2) the counterpart of *hCDC10* is expressed in the mouse, and (3) KIAA0158 is the human counterpart of the mouse *Nedd5* gene (see below). Thus the human and mouse genomes share at least four septin genes, *Diff6*, *H5*, *Nedd5*, and *CDC10*. (Note that the mammalian *CDC10* genes are not orthologs of the budding yeast *CDC10* gene.) We have been studying

Supported in part by Grants-in-Aid from the Ministry of Health and Welfare Brain Science Research Program (to MK) and the Ministry of Education, Science and Culture (to MK and MN) of Japan.

Accepted for publication August 5, 1998.

Address reprint requests to Dr. Makoto Kinoshita, Department of Molecular Oncology, Kyoto University Graduate School of Medicine, Yoshida Konoe-cho, Sakyo-ku, Kyoto 606-8501, Japan. E-mail: mkinoshi@virus.kyoto-u.ac.jp.

the mammalian septin system since we isolated the mouse *Nedd5* gene. *Nedd5* is a ubiquitous cytoskeletal component that interacts with actin-based structures such as contractile ring and stress fibers.<sup>28</sup> Recently, a set of septins were identified in a protein complex that can interact with *sec6/8* complex in the rat brain.<sup>32</sup> Since *sec6/8* complex is a cluster of molecules essential for exocytosis, another role of the septins may be to link the secretory machinery to actin-based cytoskeleton beneath plasma membrane.

In the course of screening neuropathological implications of septins based on their potential to form a filamentous complex, we tested whether they can contribute to the neurofibrillary pathology. We report here that three human septins, *Nedd5*, *Diff6*, and *H5*, are commonly deposited in and around NFTs in AD brains, whereas *hCDC10* is not. Our findings raise the possibility that at least three septins are involved in the neurodegeneration of AD by forming heteropolymer complexes which directly or indirectly interact with tau in the PHF.

## Materials and Methods

### Cases

Human brain tissue samples were obtained from the Department of Neurology, Kyoto University Hospital. Neuropathological diagnoses were based on the standard criteria for AD.<sup>33</sup> Tissues from age-matched patients without dementia-causing diseases were used as the controls. Three AD (range, 65–82 years) and 7 control (5 age-matched, range, 63–85 years; 2 young, 33 and 35 years) brain samples were analyzed by immunoblotting and reverse transcription-coupled polymerase chain reaction (RT-PCR), and five additional AD samples (range, 73–80 years) were used only for immunocytochemistry. Specimens taken from the right temporal cortices and hippocampi were quickly frozen in liquid nitrogen and then used in the biochemical analyses. Those taken from the left hemispheres were immersion-fixed and used in the histochemical analyses.

### RNA Extraction and RT-PCR

The methods have been described elsewhere.<sup>34</sup> In brief, the poly(A)<sup>+</sup> RNA (1  $\mu$ g) isolated from each hippocampal sample was reverse transcribed from an oligo-dT primer in 33  $\mu$ l of reaction medium using First Strand Synthesis Kit (Pharmacia, Uppsala, Sweden). Each sample was diluted to 1000  $\mu$ l and heat-inactivated, then 10  $\mu$ l was amplified in a 20- $\mu$ l standard PCR reaction mixture containing 0.2  $\mu$ mol/L primers (see below) and 1.25  $\mu$ Ci [ $\alpha$ -<sup>32</sup>P]dCTP under the following conditions for 20 cycles: 0.5 minute at 96°C, 0.5 minute at 52°C, and 1 minute at 72°C. Each sample was electrophoresed through a 5% polyacrylamide gel and densitometry was done with an image analyzing system, BAS2000 (Fuji, Tokyo, Japan). The amount of amplified  $\beta$ -actin gene fragment was used to estimate the amount of input cDNA for calibration. Control experiments were performed to determine the range of PCR

cycles over which amplification efficiency remained constant and to confirm that the amount of PCR product was proportional to the amount of input RNA. The identity of each PCR product was confirmed by its size and by direct sequencing. The following pairs of oligonucleotides were used as the primers (the corresponding nucleotide positions are shown in parentheses): KIAA0158/human *Nedd5*, AATCTGAGGATGAGACAGGG (2850–2869) and TGGG-TAGTAAAACCAAAGGG (3258–3277); R53785/human *Diff6*, AAGCTTTCCCGCCAGAGCGC (3–22) and CGG-GACGTGGCCTCAGAGGG (172–191); W69298/human *H5*, TCTCTGGGCAGTCAGCAGGG (31–50) and CAT-TATGGAGAACTACCGGG (379–398) S72008/*hCDC10*, CAAAGGTTCCATTCCAGTGCAGC (1720–1741) and CTCTCAAGAGGCCATGATTCC (2191–2212); X00351/human  $\beta$ -actin, AGAAGAGCTATGAGCTGCCTGACG (751–774) and TACTTGCCTCAGGAGGAGCAATG (1028–1051).

### Production and Purification of Antibodies

The production and characterization of the two anti-*Nedd5* antibodies, 6 and 11, were reported previously.<sup>28</sup> We also raised antibodies against three synthetic peptides; C10C (EQQNSSRTLEKNKKKGKIF; residues 400–418 of *hCDC10*), H5C (DFPIPAVPPGTDPE; residues in the putative product of a human cDNA clone W69298 and mouse *H5*) and D6C (TEIPLPMLPLADTE, residues corresponding to a part of the putative product of a human cDNA clone R53785, which is similar to residues 315–328 of mouse *Diff6*). Each peptide was conjugated to an equal weight of maleimide-activated bovine serum albumin (Pierce, Rockford, Illinois) via a cysteine residue added to the amino-terminus. Animals were immunized with the bovine serum albumin-conjugated antigen (0.1 mg of H5C and C10C for a guinea pig, 0.5 mg of D6C for a rabbit) emulsified in Freund's complete adjuvant (Sigma, St. Louis, MO). After boosting with Freund's incomplete adjuvant (Sigma) once or twice, collected sera were fractionated with ammonium sulfate and affinity purified using the corresponding peptides coupled with fluoromethylpyridinium toluene sulfonate-activated Cellulofine (Seikagaku, Tokyo, Japan).

### Immunoblot Analysis

We followed the standard protocols of Sambrook et al<sup>35</sup> with some modifications.<sup>28</sup> In brief, the frozen tissue samples were sonicated directly in nonreducing sodium dodecyl sulfate (SDS) buffer and then ultracentrifuged at 80,000  $\times g$  for 20 minutes. The supernatant was incubated at 100°C for 5 minutes with 2-mercaptoethanol. The lysate containing 25  $\mu$ g of total protein was separated on 10% SDS-PAGE and transferred to a polyvinylidene difluoride membrane (Micron Separations, Westborough, MA). The membrane was incubated overnight in the blocking buffer [0.2% Tween 20 in Tris-buffered saline (TBS, pH 7.4) containing 1% bovine serum albumin], then with each antibody (1  $\mu$ g/ml) in the blocking buffer for 1 hour. The membrane was washed with TBS-

Tween 20 and then incubated in the blocking buffer containing an appropriate secondary antibody conjugated with alkaline phosphatase (Chemicon, Temecula, CA, 1:5000). The immune complex was detected by a chromogenic reaction. The signals were digitized with an optical scanner, GT8000 (Epson, Tokyo, Japan), and the software NIH Image 1.55 was used for densitometry.

### Immunocytochemistry

We performed immunocytochemistry on the brain sections using rabbit polyclonal antibodies against Nedd5 (6 and 11) and Diff6 (D6C-1) and guinea pig polyclonal antibodies against H5 (H5C-1) and hCDC10 (C10C-1). Postmortem brain samples were immersion-fixed with 4% paraformaldehyde in 0.1 mol/L phosphate buffer (PB) for 24–48 hours. After cryoprotection for 48 hours in 20% sucrose in 0.1 mol/L PB, the tissues were sliced 30  $\mu\text{m}$  thick. The sections were treated for 0.5 hours with 0.5%  $\text{H}_2\text{O}_2$  in 0.1 mol/L phosphate-buffered saline (PBS, pH 7.4) containing 0.1% Triton X-100 to deplete endogenous peroxidase activities. The slides were then incubated with the primary antibodies (1  $\mu\text{g}/\text{ml}$ ) followed by biotinylated anti-rabbit IgG (Vector, Burlingame CA, 1:200) or anti-guinea pig IgG (Vector, 1:200), and the avidin-biotin-horseradish peroxidase (Vector, 1:100). The specific immune complex was detected with diaminobenzidine-nickel ammonium sulfate.

For double immunofluorescence cytochemistry of H5 (H5C-1) and either Nedd5 (antibody 6) or Diff6 (D6C-1), the sections from AD brains were incubated with each combination of the primary antibodies, then with fluorescein isothiocyanate-conjugated anti-rabbit IgG antibody (Chemicon, 10  $\mu\text{g}/\text{ml}$ ) and biotinylated anti-guinea pig IgG antibody (Vector, 1:200), followed by treatment with Texas Red-conjugated avidin (Vector, 1:1000). For double staining of phosphorylated tau (Tau2, Sigma, 1:1000 or AT8, Innogenetics, Zwijndrecht, Belgium, 1:1000) and either of Nedd5 (6), H5 (H5C-1) or Diff6 (D6C-1), we used fluorescein isothiocyanate-conjugated anti-mouse IgG (Chemicon, 10  $\mu\text{g}/\text{ml}$ ) and biotinylated antibodies (ie, anti-rabbit IgG for Nedd5 and Diff6, and anti-guinea pig IgG for H5, Vector, 1:200) with Texas Red-conjugated avidin (Vector, 1:1000). The sections were observed through the appropriate filters.

Double staining for C4d and septins were done as follows: Sections were sequentially incubated with mouse monoclonal antibody against C4d (Quidel, San Diego, CA, 1:1000) and the biotinylated secondary antibody and developed for 10 minutes in a solution containing 0.02% diaminobenzidine and 150  $\mu\text{mol}/\text{L}$   $\text{H}_2\text{O}_2$  in 50 mmol/L Tris-Cl (pH 7.6). After incubation in 150 mmol/L  $\text{H}_2\text{O}_2$  in PBS for 30 minutes, the sections went through the second staining cycle with each of the anti-septin antibodies and biotinylated secondary antibody, then they were developed in 0.02% diaminobenzidine and 0.6% nickel ammonium sulfate solution. Consequently, C4d was stained brown and septins were labeled dark purple.

### Immunoelectron Microscopy

A pre-embedding method was used for the immunoelectron microscopy. Paraformaldehyde-fixed entorhinal cortices from AD patients were sectioned (50  $\mu\text{m}$  thick) in a vibratome. The sections were blocked with 20% normal goat serum for 1 hour and then incubated with anti-Nedd5 antibodies (6 or 11, 1  $\mu\text{g}/\text{ml}$ ) in 0.1 mol/L PB overnight at 4°C, followed by incubation with 1.4 nm gold-coupled anti-rabbit IgG (Nanoprobes, Stony Brook, NY, 1:100). Sections were postfixed in 1% glutaraldehyde in distilled water for 10 minutes. The sections were treated with HQ Silver enhancement kit (Nanoprobes), then with 1%  $\text{OsO}_4$  in 0.1 mol/L PB, stained with 1% uranyl acetate, dehydrated in ethanol, and flat-embedded in epoxy resin. Serial ultrathin sections 50 nm thick were observed with an H-7100 electron microscope (Hitachi, Tokyo, Japan).

### Results

#### Expression of Human Septin Genes in the Brain

The complete human septin cDNA sequences of KIAA0158 (encoding the human counterpart of mouse Nedd5, which we call human Nedd5 in this paper) and *hCDC10* are available in the database. In addition, there are partial human cDNA sequences (eg, accession nos. R36763 and W69298) encoding polypeptides that are 85% and 94% identical to the amino- and carboxy-terminal sequences, respectively, of mouse H5. Likewise, we found several other human cDNAs (eg, accession nos. AA262134 and R53785) encoding polypeptides that are 96% and 98% identical to the middle and carboxy-terminal portions, respectively, of mouse Diff6. Given the high interspecies conservation of the amino acid sequences of the septin counterparts (eg, 99% between human and mouse Nedd5) and the moderate amino acid identities (50–60%) shared among the septins in a given mammalian species,<sup>18</sup> these cDNA fragments are likely to be derived from the human counterparts of the mouse *H5* and *Diff6* genes. In this study, we have therefore regarded R36763/W69298 and AA262134/R53785 as partial cDNA fragments of the human *H5* and *Diff6* genes, respectively.

We assessed expression of the four human septin genes (*Nedd5*, *hCDC10*, *H5*, and *Diff6*) in postmortem brain samples using RT-PCR analysis. We found that the four septin genes were expressed in all of the brain samples investigated in this study: AD ( $n = 3$ ), age-matched control ( $n = 5$ ), and young control ( $n = 2$ ) brains (Figure 1a). The identity of each PCR product was confirmed by size and DNA sequence. Densitometric data of each septin gene's expression level in the three groups were as follows (standardized with the  $\beta$ -actin gene expression level, arbitrary unit): *Nedd5* (AD  $101 \pm 7$ , age-matched  $106 \pm 12$ , young  $119 \pm 11$ ), *hCDC10* ( $108 \pm 3$ ,  $119 \pm 8$ ,  $146 \pm 16$ ), *H5* ( $122 \pm 5$ ,  $107 \pm 4$ ,  $121 \pm 1$ ), *Diff6* ( $130 \pm 2$ ,  $125 \pm 4$ ,  $135 \pm 16$ ). We could not detect any consistent differences in the expression levels among these limited number of samples.

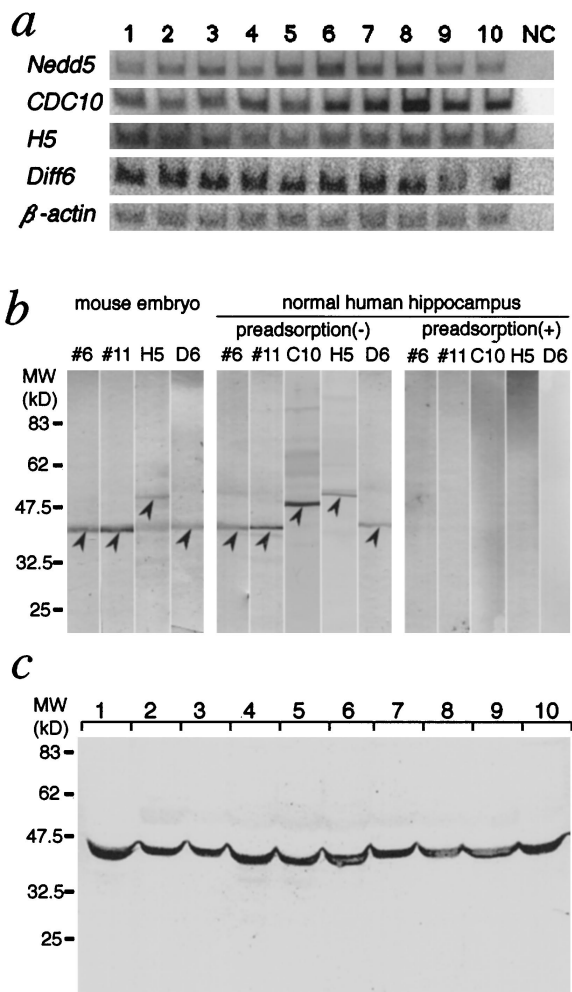


**Figure 1.** Expression of the four septins in AD and control brains. **a:** RT-PCR analysis of the human septin genes expressed in the hippocampus. Poly(A)<sup>+</sup> RNA (~10 ng) from human hippocampal regions was reverse-transcribed and subjected to PCR using primer sets for human *Nedd5*, *Diff6*, *H5*, and *hCDC10*, and for  $\beta$ -actin as an internal control. Representative results for AD brains (lanes 1–3), age-matched (lanes 4–7, 10) and young (lanes 8, 9) control brains, and a negative control without template cDNA (NC) are shown. **b:** Characterization of the four anti-septin antibodies used in this study. Each antibody (6 and 11 for *Nedd5*, H5C-1 for *H5*, and D6C-1 for *Diff6*) was tested by immunoblotting of lysates from mouse embryos (at gestational day 13.5) and a normal human hippocampus. Each lane contained 25  $\mu$ g of total protein. Immunoreactive bands (arrowheads) were abolished when antibodies preadsorbed with the corresponding antigens were used. **c:** Immunoblot of the hippocampal lysates of AD and control brains. A representative blot showing *Nedd5* (detected by antibody 11) in brains from AD patients (lanes 1–3), age-matched controls (lanes 4–7, 10) and the young individuals (lanes 8, 9). Each lane contained 25  $\mu$ g of total protein.

### Characterization of the Septin Antibodies

We raised polyclonal antibodies against the four mammalian septins (*Nedd5*, *H5*, *Diff6* and *CDC10*) using recombinant proteins or synthetic peptides that correspond to amino acid sequences highly conserved between the human and mouse counterparts but distinct from the other septins. Authenticity of the two antibodies (6 and 11) that recognize distinct regions of human/mouse *Nedd5* was established previously.<sup>28</sup> Three other anti-

bodies were raised against synthetic peptides corresponding to portions near the carboxy-termini of *H5*, *Diff6*, and *CDC10* (*H5C-1*, *D6C-1*, *C10C-1*), respectively. These sequences were not shared by any other polypeptide in the database.

Using these antibodies, we performed immunoblot analysis with mouse embryonic and human brain tissues. As we reported previously,<sup>28</sup> the two anti-*Nedd5* antibodies detected 41.5-kd proteins both in the mouse and human tissues. These bands were abolished after treatment of each antibody with excess corresponding antigen (Figure 1b). Likewise, each of the antibodies *H5C-1*, *D6C-1*, and *C10C-1* detected a single band of expected size (54, 42, and 49 kd, respectively) in the human and mouse tissue samples (Figure 1b). Each band was abolished by preadsorption with excess amount of the corresponding antigen but not with the other septin antigens (Figure 1b and data not shown). These results established that each antibody reacted specifically with the corresponding human septins in the brain samples without mutual cross-reactivity. The molecular weights of the putative human *H5*, *Diff6* and *hCDC10* estimated by the immunoblotting are comparable to those of the mouse homologs, providing additional evidence of their identity as the human counterparts.

We assessed the amount of *Nedd5* in SDS-soluble fractions of the hippocampal and temporal cortices from AD ( $n = 3$ ), age-matched control ( $n = 5$ ), and young control ( $n = 2$ ) brains. Densitometric analysis of the bands showed no consistent differences among the groups; AD  $116 \pm 16$ , age-matched  $145 \pm 20$ , young  $136 \pm 13$  (Figure 1c).

### Detection of Septins in Brain Tissue Sections

We immunostained paraformaldehyde-fixed, free-floating tissue sections from histopathologically confirmed AD brains ( $n = 8$ ) as well as those of age-matched ( $n = 5$ ) and young ( $n = 2$ ) control cases. Anti-*Nedd5* antibody 6 labeled numerous NFTs and neuropil threads in the entorhinal cortex of AD brains (Figure 2a). Positive staining was completely abolished by preadsorption of the antibodies with excess antigens but was not affected by preadsorption with antigens of the other septins (Figure 2, a and b, and data not shown). Elimination of the primary antibodies also abolished the signals. In contrast, these antibodies did not label obvious structures more than diffuse cytoplasmic staining in the young control brains (Figure 2c and data not shown). In AD brains, antibodies 6 and 11 against *Nedd5* consistently stained NFTs (Figure 2, d and e). *Nedd5* was also detected in neurites in the neuropil (neuropil threads) and dystrophic neurites in senile plaques of AD brains (Figure 2a). These *Nedd5*-positive structures were abundant, particularly in the hippocampus and entorhinal cortex. Antibodies against *H5* (*H5C-1*) and *Diff6* (*D6C-1*) gave essentially the same staining patterns as those of 6 and 11, whereas an antibody against *hCDC10* (*C10C-1*) did not label NFTs (Figure 2, f and g, and data not shown). NFTs sparsely distributed in the age-matched entorhinal cortices were

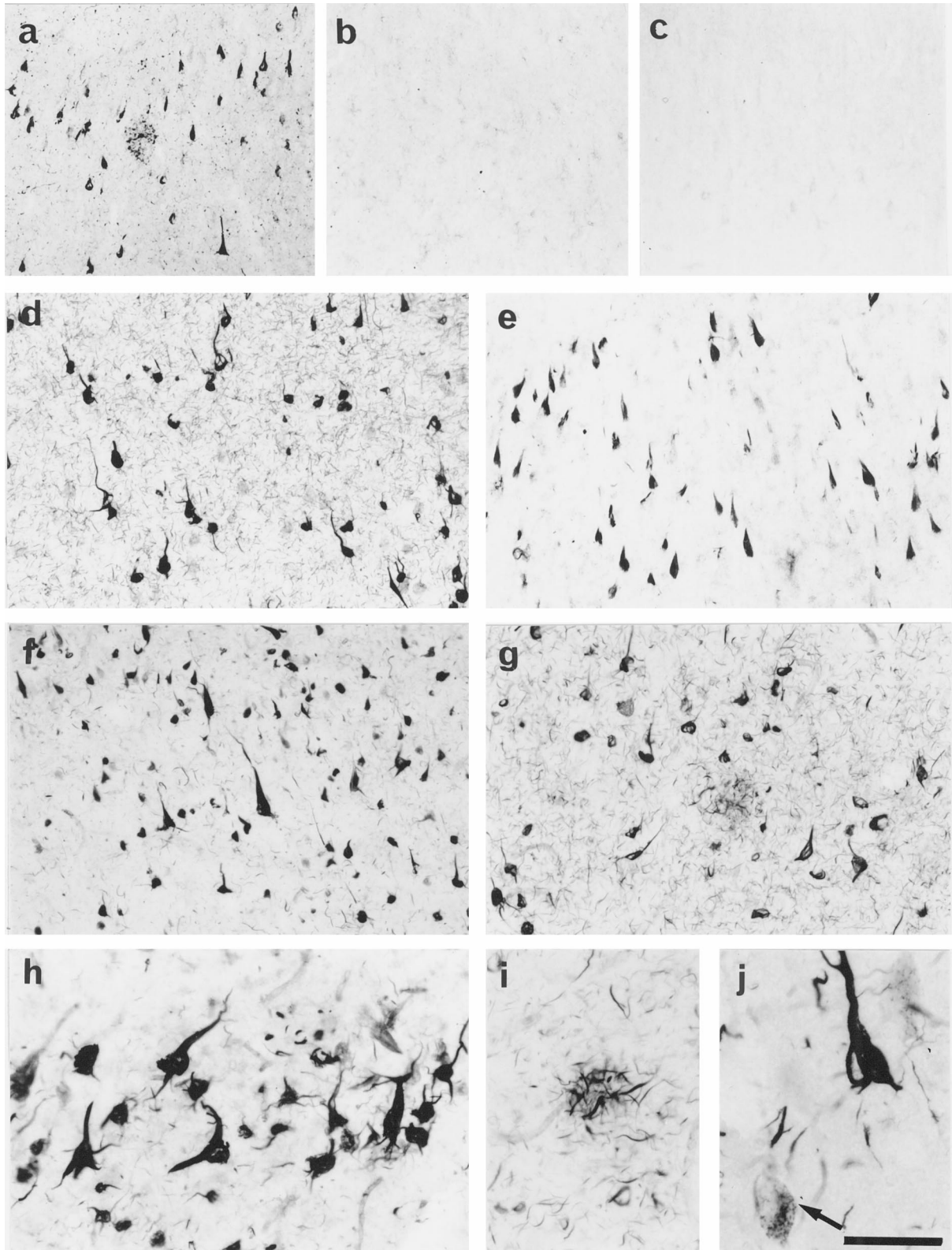


**Figure 2.** Immunocytochemical detection of septins in AD and control brains. **a:** Anti-Nedd5 antibody 6 labeled numerous NFTs, neuropil threads and dystrophic neurites in the senile plaques in the entorhinal cortex of an AD brain. **b:** Preadsorption of 6 with the antigen peptide abolished the signals on an adjacent section from the same patient as in **a**. **c:** A representative section of the entorhinal cortex from a young individual showing minimal cytoplasmic staining for Nedd5. **d** to **g:** Sections of the entorhinal cortex and hippocampus from AD brains immunostained with the following anti-septin antibodies; 6 (**d**) and 11 (**e**) for Nedd5, H5C-1 (**f**) for H5, and D6C-1 (**g**) for Diff6. NFTs, neuropil threads, and dystrophic neurites are intensely labeled with the four antibodies but the normal-appearing neurons are not stained. **h** to **j:** Higher magnifications of the immunolabeled AD brain sections. NFTs, neuropil threads (**h**), and dystrophic neurites of senile plaque (**i**) are intensely stained with anti-Nedd5 antibody 6. Some glial tangles are also seen in **h**. In **j**, H5-immunoreactive granules (pre-tangles) beside the manifest NFT in the neuronal cytoplasm are shown (arrow). Scale: 200  $\mu\text{m}$  (**a-c**), 130  $\mu\text{m}$  (**d, e**), 100  $\mu\text{m}$  (**f, g**), 50  $\mu\text{m}$  (**h-j**).

also stained for Nedd5, H5, and Diff6, but not for hCDC10 (data not shown).

The three septins (Nedd5, H5 and Diff6) were also detected in the cytoplasm of a small number of neurons that did not manifest NFTs, where immunoreactivities were distributed in a granular pattern (Figure 2j and data not shown), probably corresponding to the pre-tangles (also referred to as stage 0 tangles<sup>36</sup> or Group 1 tangles<sup>37</sup>).

Septin-positive fibrous structures, which appear to be glial tangles in astrocytes, were also found in small non-pyramidal cells in AD brains (Figure 2h).

### *Colocalization of Septins and Tau in Intracellular NFTs*

*Drosophila* and rat septins are known to form heteropolymer complexes *in vivo*.<sup>23,24,32</sup> However, we found that tissue distribution and subcellular localization of Nedd5, H5, Diff6, and CDC10 in mouse and human cells are not necessarily identical (Kinoshita, Valencik, Kinoshita, Pringle, and Noda, manuscript in preparation). Thus we tested colocalization of the septins in NFTs. Double immunofluorescence staining of the hippocampus and entorhinal cortex of AD brains showed largely overlapping labeling patterns for H5 and Diff6 (Figure 3, a and b), except for a few Diff6-positive NFTs that were H5-negative (arrowheads in Figure 3b). Similar results were obtained for the combination of Nedd5 and H5 (data not shown). We then compared localization of the septins and tau, the major constituent of NFTs. For instance, double labeling of AD hippocampi for Diff6 (with D6C-1 antibody) and phosphorylated tau (with commercial antibodies Tau2 or AT8) showed that roughly 95% of NFTs were doubly labeled for both tau and Diff6 (Figure 3, c and d). We therefore concluded that the septins localize close to the phosphorylated tau in the majority of NFTs. Interestingly, however, some other neurons appeared to contain almost exclusively either tau (Figure 3f) or Diff6 (Figure 3e). Even in the double-positive neurons, subcellular distributions of Diff6 and tau appear overlapping but not identical (Figure 3, c and d): tau is enriched both in somatic and dendritic NFTs, whereas Diff6 appears to localize more proximally (see Discussion). These data also support the observation that the antibodies are not mutually cross-reactive.

After disintegration of tangled neurons, NFTs are known to remain *in situ* and exposed to the extracellular milieu. These extracellular NFTs (eNFTs) have a unique immunocytochemical profile: ie, a number of tau epitopes have been lost, probably through proteolytic processing. Meanwhile, activation of the complement system takes place against eNFTs, resulting in heavy decoration with various complement proteins.<sup>38</sup> Our double-staining analysis showed that the distribution patterns of septin-positive NFTs and complement C4d-positive NFTs (eNFTs) were mutually exclusive (Figure 3g). These findings indicate that septin-positive NFTs are formed intracellularly and that the septin epitopes may be lost due to

proteolytic degradation or other modifications after neuronal collapse.

### *Electron Microscopic Detection of a Septin in PHF*

Ultrastructural localization of a septin in the NFTs was analyzed in the entorhinal cortex of AD patients using a pre-embedding, immunogold-labeling method by using anti-Nedd5 antibodies (6 and 11). Both of the two antibodies gave specific labeling along PHFs (Figure 4, a and b, and data not shown). No labeling was detected in association with neurofilaments, glial fibrils or any other normal structures in the cytoplasm.

### *Discussion*

We showed that the three human septins, Nedd5, H5 and Diff6, are concentrated in intracellular NFTs, dystrophic neurites in senile plaques, neuropil threads in the brains of all of the AD patients studied and, to a much lesser extent, in some elderly controls. It is unlikely that staining was due to nonspecific labeling or cross-reactivity to other proteins, in particular the major NFT component tau, for three reasons: (1) none of the known septins shares similarities in the primary structure with tau; (2) the results were consistent with antibodies directed against two distinct epitopes in Nedd5; and (3) double staining with each septin and tau revealed a minor but obvious dissociation in their localization.

As assessed by the RT-PCR and immunoblot analyses, brains from young individuals contain as much septin mRNAs and their products as AD brains. By immunocytochemistry, however, no obvious structure more than diffuse cytoplasmic staining was found in young brains (Figure 2b). We are not sure of the specificity of this staining because the signal intensity is as weak as the background level of preadsorbed one (Figure 2c). Such discrepancy between the immunoblot and immunocytochemistry results is reminiscent of the case of tau.<sup>39</sup> In normal neurons, tau is distributed along microtubules or diffusely in the cytoplasm, which is barely detectable with current immunocytochemical techniques. Tau becomes detectable only at high concentrations in the neurofibrillary changes. Similar explanation may apply to the septins. In addition, certain conformational changes through the aggregation process might enhance immunoreactivity, as has been proposed for anti-tau antibodies, Alz-50 and MC-1.<sup>40</sup> Our negative results with an anti-hCDC10 antibody could be explained by reduced immunoreactivity after conformational changes or epitope masking through complex formation. Alternatively, hCDC10 may be in fact excluded from NFT because isoelectric points of Nedd5, Diff6, and H5 are 6.2, 5.6, and 5.5, respectively, whereas those of hCDC10 and tau are 9.0 and 9.9. Thus, the three acidic septins can be highly interactive with extremely basic protein tau, while a basic septin hCDC10 cannot.

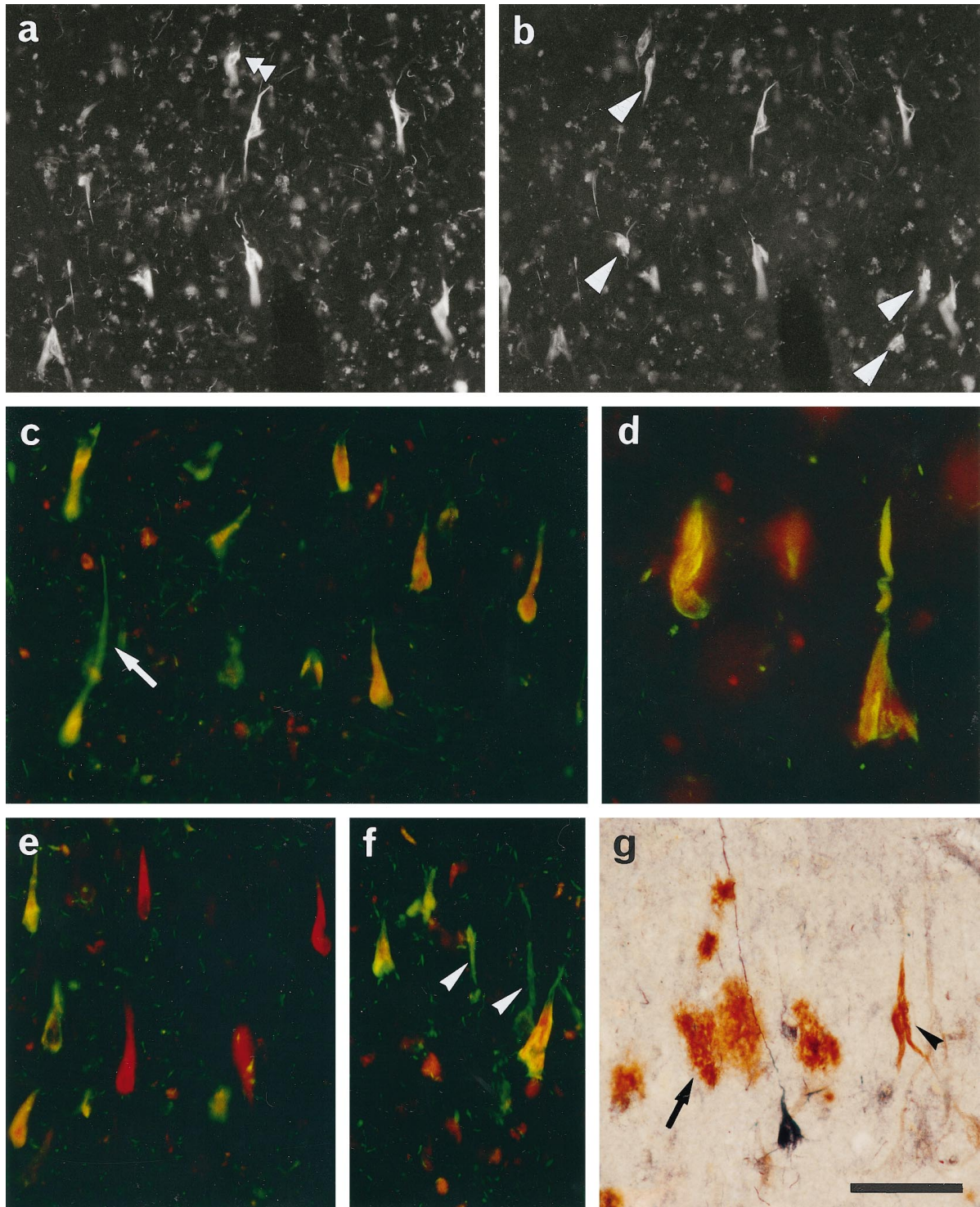


**Figure 3.** Double immunolabeling analyses of the entorhinal cortices from AD brains. **a** and **b**: H5 (**a**) and Diff6 (**b**) were labeled respectively with Texas Red and fluorescein. Signals for H5 and Diff6 largely overlap in the NFTs. However, a few NFTs are positive exclusively for H5 (**double arrowhead**) or Diff6 (**arrowheads**). **c–f**: Tau and Diff6 were labeled respectively with fluorescein (**green**) and Texas Red (**red**). The two signals were largely colocalized (shown as **yellow** in **c, d**), but found dissociated in some cases; ie, red cells (**e**) and green cells (**f**) (**arrowheads**). Note their distinct subcellular distribution in a single neuron (**arrow** in **c, d**). **g**: C4d and Nedd5 (**6**) were labeled brown and dark purple, respectively. Note that C4d-positive extracellular NFTs contain little, if any, immunoreactivity for Nedd5 (**arrowhead**). Diffuse plaques are intensely stained for C4d but not for Nedd5 (**arrow**). Scale: 100  $\mu\text{m}$ .

The three septins exist not only in typical NFTs but in granular or fine fibrillar deposits in the neuronal soma as well. These structures may be considered as the earliest detectable stage of NFT formation (stage 0 tangles<sup>36</sup> or

Group 1 tangles<sup>37</sup>). These changes were not found in young control brains, but were sparsely present in elderly controls. This may reflect the fact that degenerative neuronal changes accompanied by NFTs also develop, to a

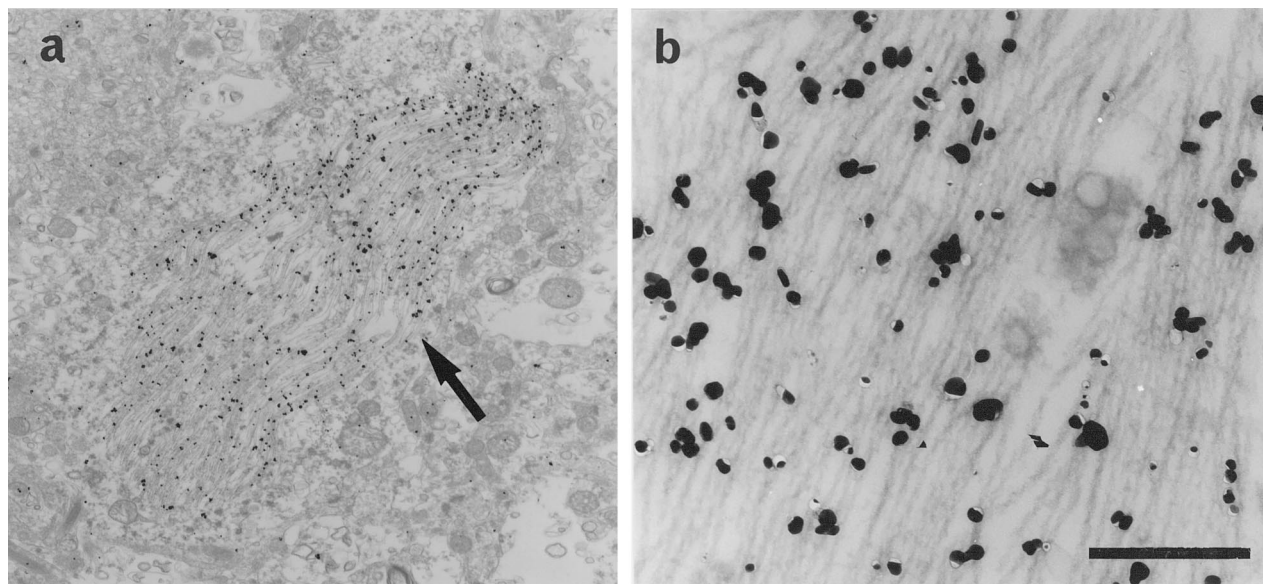


**Figure 4.** Immunoelectron micrographs for Nedd5 in the entorhinal cortex of an AD brain. **a:** An electron micrograph showing that gold particles for Nedd5 (arrow) specifically labeled NFTs in the neuronal cytoplasm. Scale: 4  $\mu\text{m}$ . **b:** A higher magnification of the NFTs. The gold particles are concentrated along PHFs in the cytoplasm. Scale: 0.4  $\mu\text{m}$ .

much lesser extent, with normal aging.<sup>41</sup> The presence of septins in such pre-tangles indicates that precursory, septin-containing aggregates are formed diffusely in the cytoplasm during the latent or earliest stage of NFT formation. The dissociation of immunoreactivities for septins and tau in a minor fraction of tangled neurons (Figure 3, e and f) may be attributable to masking of the epitopes by steric hindrance or secondary modification. However, the composition of Diff6-positive, phosphorylated tau-negative NFT-like structures (Figure 3e) would be intriguing because such accumulation of septins might be a novel mode of neurodegeneration.

Ample evidence has established that hyperphosphorylated tau is the major constituent of PHFs.<sup>15</sup> Because hyperphosphorylation of tau reduces its affinity for microtubules, it has been postulated that the increased unbound tau in the cytoplasm aggregates into PHFs. However, failure of tau-overexpressing transgenic mice to develop neurofibrillary changes<sup>42</sup> suggests that additional factors are required to promote NFT/PHF formation. On the other hand, extracellular accumulation of amyloid  $\beta$  protein ( $A\beta$ ) is considered as a major factor in AD, but transgenic mice that overexpress  $\beta\text{PP}$  or its variants do not develop NFTs despite heavy  $A\beta$  deposits in the brain.<sup>43,44</sup> Such diseases as dementia pugilistica, viral encephalitis (subacute sclerosing panencephalitis), Guam Parkinson-dementia complex,<sup>45</sup> Niemann-Pick disease type C,<sup>46</sup> and myotonic dystrophy<sup>47</sup> show neurofibrillary pathology without marked  $A\beta$  deposits. These data indicate that diverse factors can trigger NFT formation as a final common pathway; however, tau is not sufficient and  $A\beta$  deposition is not necessary.

We have demonstrated that Nedd5, hCDC10, H5, and Diff6 are associated with actin cytoskeleton and recruited in the neurite and growth cone<sup>28</sup> (Kinoshita, Valencik,

Kinoshita, Pringle, and Noda, manuscript in preparation). Recently, a fraction of septins in the cytoplasm have been identified in a complex that interacts with the sec6/8 complex in the rat brain.<sup>32</sup> Although physiological functions of the septin complex in the mammalian brain are yet to be determined, these and other data obtained in other species<sup>18,21,23</sup> suggest that mammalian septins provide scaffolds for organization of submembranous structures, neuronal polarity, and vesicle trafficking. We have previously shown that the assembly of septin filament is regulated by several factors such as growth signals, actin filament, and GTP hydrolysis, and that direct and indirect disturbances of these factors result in abnormal distribution and aggregation of Nedd5.<sup>28</sup> Therefore, whatever the original pathogenetic factors may be, disturbed septin assembly in neurons may affect the vesicular transport and structural integrity, eventually accelerating the degenerative processes.

Septins are also present in glial tangles in some degenerating astrocytes (Figure 2h). We also observed septin-positive glial tangles in the brains of multiple system atrophy patients (unpublished data). Thus involvement of septins in the pathological structures may be a common degenerative process in neuronal and glial lineages across distinct disease entities.

We found that overexpression of *Nedd5* in cultured cells gives rise to septin-containing fibrous or flame-shaped deposits in the cytoplasm (unpublished data). This suggests that excessive and/or disproportional aggregation of septin monomers in the cytoplasm can provide scaffolds for further recruitment of proteins such as septins and tau, promoting formation of pre-tangles and, subsequently, of NFTs. Testing whether the septin scaffolds accelerate the organization of tau into NFTs, or vice versa, should provide important insights into the molec-



ular mechanisms of NFT formation and the neuronal defects in AD.

### Acknowledgments

We thank Ms. M. Fukuda, K. Imai, and A. Miyazaki for technical and/or secretarial assistance.

### References

1. Yankner BA, Mesulam MM: Seminars in medicine of the Beth Israel Hospital, Boston. Beta-amyloid and the pathogenesis of Alzheimer's disease. *N Engl J Med* 1991, 325:1849-1857
2. McKee AC, Kosik KS, Kowall NW: Neuritic pathology and dementia in Alzheimer's disease. *Ann Neurol* 1991, 30:156-165
3. Arriagada PV, Growdon JH, Hedley-White T, Hyman BT: Neurofibrillary tangles but not senile plaques parallel duration and severity of Alzheimer's disease. *Neurology* 1992, 42:631-639
4. Xu Z, Cork LC, Griffin JW, Cleveland DW: Increased expression of neurofilament subunit NF-L produces morphological alterations that resemble the pathology of human motor neuron disease. *Cell* 1993, 73:23-33
5. Côté F, Collard J-F, Julien J-P: Progressive neuropathy in transgenic mice expressing the human neurofilament heavy gene: a mouse model of amyotrophic lateral sclerosis. *Cell* 1993, 73:35-46
6. Yankner BA: New clues to Alzheimer's disease: Unraveling the roles of amyloid and tau. *Nature Med* 1996, 2:850-852
7. Kidd M: Paired helical filaments in electron microscopy of Alzheimer's disease. *Nature* 1963, 197:192-193
8. Braak H, Braak E, Grundke-Iqbal I, Iqbal K: Occurrence of neurofibrillary threads in the senile human brain and in Alzheimer's disease: a third location of paired helical filaments outside of neurofibrillary tangles and neuritic plaques. *Neurosci Lett* 1986, 65:351-355
9. Grundke-Iqbal I, Iqbal K, Quinlan M, Tung Y-C, Zaidi MS, Wisniewski HM: Microtubule-associated protein tau: a component of Alzheimer paired helical filaments. *J Biol Chem* 1986, 261:6084-6089
10. Kosik KS, Joachim CL, Selkoe DJ: The microtubule-associated protein tau is a major antigenic component of paired helical filaments in Alzheimer's disease. *Proc Natl Acad Sci USA* 1986, 83:4044-4048
11. Wood JG, Mirra SS, Pollock NJ, Binder LI: Neurofibrillary tangles of Alzheimer's disease share antigenic determinants with the axonal microtubule-associated protein tau. *Proc Natl Acad Sci USA* 1986, 83:4040-4043
12. Goedert M, Wischik CM, Crowther RA, Walker JE, Klug A: Cloning and sequencing of the cDNA encoding a core protein of the paired helical filament of Alzheimer's disease: identification as the microtubule-associated protein tau. *Proc Natl Acad Sci USA* 1988, 85:4051-4055
13. Kondo J, Honda T, Mori H, Hamada Y, Miura R, Ogawara M, Ihara Y: The carboxyl third of tau is tightly bound to paired helical filaments. *Neuron* 1988, 1:827-834
14. Wischik CM, Novak M, Thøgersen HC, Edwards PC, Runswick MJ, Jakes R, Walker JE, Milstein C, Roth M, Klug A: Isolation of a fragment of tau derived from the core or the paired helical filament of Alzheimer's disease. *Proc Natl Acad Sci USA* 1988, 85:4506-4510
15. Morishima-Kawashima M, Hasegawa M, Takio K, Suzuki M, Yoshida H, Watanabe A, Titani K, Ihara Y: Hyperphosphorylation of tau in PHF. *Neurobiol Aging* 1995, 16:365-380
16. Mori H, Kondo J, Ihara Y: Ubiquitin is a component of paired helical filaments in Alzheimer's disease. *Science* 1987, 235:1641-1644
17. Wang J-H, Grundke-Iqbal I, Iqbal K: Glycosylation of microtubule-associated protein tau: An abnormal posttranslational modification in Alzheimer's disease. *Nature Med* 1996, 2:871-875
18. Longtine MS, DeMarini DJ, Valencik ML, Al-Awar OS, Fares H, DeVirgilio C, Pringle JR: The septins: roles in cytokinesis and other processes. *Curr Opin Cell Biol* 1996, 8:106-119
19. Cooper JA, Kiehart DP: Septins may form a ubiquitous family of cytoskeletal filaments. *J Cell Biol* 1996, 134:1345-1348
20. Byers B: The molecular biology of the yeast *Saccharomyces*. *Life Cycle and Inheritance*. Edited by Strathern JN, Jones EW, Broach JR. Vol. 1. Cold Spring Harbor, NY, Cold Spring Harbor Laboratory Press, 1981, pp 59-96
21. Chant J: Septin scaffolds and cleavage planes in *Saccharomyces*. *Cell* 1996, 84:187-190
22. Neufeld TP, Rubin GM: The *Drosophila* peanut gene is required for cytokinesis and encodes a protein similar to yeast putative bud neck filament proteins. *Cell* 1994, 77:371-379
23. Fares H, Peifer M, Pringle JR: Localization and possible functions of *Drosophila* septins. *Mol Biol Cell* 1995, 6:1843-1859
24. Field CM, Al-Awar O, Rosenblatt ML, Alberts BM, Mitchison TJ: A purified *Drosophila* septin complex forms filaments, and exhibits GTPase activity. *J Cell Biol* 1996, 133:605-616
25. Nottenburg C, Gallatin WM, St. John T: Lymphocyte HEV adhesion variants differ in the expression of multiple gene sequences. *Gene* 1990, 95:279-284
26. Kato K: A collection of cDNA clones with specific expression patterns in mouse brain. *Eur J Neurosci* 1990, 2:704-711
27. Kumar S, Tomooka Y, Noda M: Identification of a set of genes with developmentally down-regulated expression in the mouse brain. *Biochem Biophys Res Commun* 1992, 185:1155-1161
28. Kinoshita M, Kumar S, Mizoguchi A, Ide C, Kinoshita A, Haraguchi T, Hiraoka Y, Noda M: Nedd5, a mammalian septin, is a novel cytoskeletal component interacting with actin-based structures. *Genes Dev* 1997, 11:1535-1547
29. Nakatsuru S, Sudo K, Nakamura Y: Molecular cloning of a novel human cDNA homologous to CDC10 in *Saccharomyces cerevisiae*. *Biochem Biophys Res Commun* 1994, 202:82-87
30. Nagase T, Seki N, Tanaka A, Ishikawa K, Nomura N: Prediction of the coding sequences of unidentified human genes. IV. The coding sequences of 40 new genes (K1AA0121-K1AA0160) deduced by analysis of cDNA clones from human cell line KG-1. *DNA Res* 1995, 2:167-174
31. Zieger B, Hashimoto Y, Ware J: Alternative expression of platelet glycoprotein Ib( $\beta$ ) mRNA from an adjacent 5' gene with an imperfect polyadenylation sequence. *J Clin Invest* 1997, 99:520-525
32. Hsu S-C, Hazuka CD, Roth R, Foletti DL, Heuser J, Scheller RH: Subunit composition, protein interaction and structures of the mammalian brain sec6/8 complex and septin filaments. *Neuron* 1998, 20:1111-1122
33. Mirra SS, Hart MN, Terry RD: Making the diagnosis of Alzheimer's disease. A primer for practicing pathologists. *Arch Pathol Lab Med* 1993, 117:132-144
34. Kinoshita M, Tomimoto H, Kinoshita A, Kumar S, Noda M: Up-regulation of the *Nedd2* gene encoding an ICE/Ced-3-like cysteine protease in the gerbil brain after transient global ischemia. *J Cereb Blood Flow Metab* 1997, 17:507-514
35. Sambrook J, Fritsch EF, Maniatis T: *Molecular Cloning: A Laboratory Manual* (2nd ed.) Cold Spring Harbor, NY, Cold Spring Harbor Laboratory Press, 1989
36. Bancher C, Brunner C, Lassmann H, Budka H, Jellinger K, Wiche G, Seitelberger F, Grundke-Iqbal I, Iqbal K, Wisniewski HM: Accumulation of abnormally phosphorylated tau protein precedes the formation of neurofibrillary tangles in Alzheimer's disease. *Brain Res* 1989, 477:90-99
37. Braak E, Braak H, Mandelkow E-M: A sequence of cytoskeleton changes related to the formation of neurofibrillary tangles and neurofibrillary threads. *Acta Neuropathol* 1994, 87:554-567
38. McGeer PL, Akiyama H, Itagaki S, McGeer EG: Immune system response in Alzheimer's disease. *Can J Neurol Sci* 1989, 16:516-527
39. Wolozin B, Davies P: Alzheimer-related neuronal protein A68: specificity and distribution. *Ann Neurol* 1987, 22:521-526
40. Jicha GA, Bowser R, Kazam IG, Davies P: Alz-50 and MC-1, a new monoclonal antibody raised to paired helical filaments, recognized conformational epitopes on recombinant tau. *J Neurosci Res* 1997, 48:128-132
41. Dickson DW, Crystal HA, Mattiace LA, Masur DM, Blau AD, Davies P, Yen SH, Aronson MK: Identification of normal and pathological aging in prospectively studied nondemented elderly humans. *Neurobiol Aging* 1992, 13:1-11
42. Götz J, Probst A, Spillantini MG, Schäfer T, Jakes R, Bürki K, Goedert M: Somatodendritic localization and hyperphosphorylation of tau protein in transgenic mice expressing the longest human brain tau isoform. *EMBO J*, 1995, 14:1304-1313
43. Games D, Adams D, Alessandrini R, Barbour R, Berthelette P, Black-

- well C, Carr T, Clemens J, Donaldson T, Gillespie F, Guido T, Hago-  
pian S, Johnson-Wood K, Khan K, Lee M, Leibowitz P, Lieberburg I,  
Little S, Masliah E, McConlogue L, Montoya-Zavala M, Mucke L,  
Paganini L, Penniman E, Power M, Schenk D, Seubert P, Snyder B,  
Soriano F, Tan H, Vitale J, Wadsworth S, Wolozin B, Zhao J: Alzhei-  
mer-type neuropathology in transgenic mice overexpressing V717F  
 $\beta$ -amyloid precursor protein. *Nature* 1995, 373:523-527
44. Hsiao K, Chapman P, Nilsen S, Eckman C, Harigaya Y, Younkin S,  
Yang F, Cole G: Correlative memory deficits, A $\beta$  elevation and amy-  
loid plaques in transgenic mice. *Science* 1996, 274:99-102
45. Wisniewski K, Jervis GA, Moretz RC, Wisniewski HM: Alzheimer neu-  
rofibrillary tangles in diseases other than senile and presenile demen-  
tia. *Ann Neurol* 1979, 5:288-294
46. Suzuki K, Parker CC, Pentchev PG, Katz D, Ghetti B, D'Agostino AN,  
Carstea ED: Neurofibrillary tangles in Niemann-Pick disease type C.  
*Acta Neuropathol* 1995, 89:227-238
47. Kiuchi A, Otsuka N, Namba Y, Nakano I, Tomonaga M: Presenile  
appearance of abundant Alzheimer's neurofibrillary tangles without  
senile plaques in the brain in myotonic dystrophy. *Acta Neuropathol*  
1991, 82:1-5
48. Neve RL, Robakis NK: Alzheimer's disease: a re-examination of the  
amyloid hypothesis. *Trends Neurosci* 1998, 21:15-19